Journal of Surface Analysis, Vol. 25 No. 3 (2019) pp. 172 - 180
K. Matsumura, et al., Development of Secondary Ion Optical System to Achieve Three-Dimensional Shave-off SIMS
https://doi.org/10.1384/jsa.25.172

Paper

Development of Secondary Ion Optical System to Achieve Three-Dimensional Shave-off SIMS

Kohei Matsumura,[1,*] So-Hee Kang,[1] Bunbunoshin Tomiyasu,[2] and Masanori Owari[1, 2]
[1] *Institute of Industrial Science, The University of Tokyo, 4-6-1 Komaba, Meguro-ku, Tokyo 153-8505, Japan*
[2] *Environmental Science Center, The University of Tokyo, 7-3-1 Hongo, Bunkyo-ku, Tokyo 113-0033, Japan*
[*] *ko-matsu@iis.u-tokyo.ac.jp*

(Received: December 5, 2018; Accepted: February 10, 2019)

Secondary ion mass spectrometry (SIMS) has some disadvantages including degradation in depth resolution depending on the depth which are difficult to resolve. To address these disadvantages, we have previously developed shave-off SIMS and achieved two-dimensional mapping. In this study, we designed the appropriate secondary ion optical system by simulation to achieve three-dimensional shave-off SIMS. We developed new optical parts and evaluated the abilities of the designed secondary ion optical system. We acquired the following abilities of the secondary ion optical system: magnification ratio 1.6×10^2, Z-axial resolution 0.70 μm, and transmission > 0.1%.

1. Introduction

Secondary ion mass spectrometry (SIMS) is a surface analytical technique with some unique advantages. However, it has some disadvantages that are difficult to resolve, such as shape and material dependence of sputtering yield and structural damage occurring on the sample surface. To resolve or lessen these issues, we developed a new method called "shave-off SIMS" [1-3]. In conventional SIMS, the primary ion beam scans just on the surface, and the depth information is acquired by repeating XY scanning (Fig. 1a). In shave-off SIMS, the primary ion beam scans on the XY plane and shaves off the entire cross section (XZ plane) of the sample (Fig. 1b). The entire analysis is completed by only one shave-off SIMS procedure. Thus, the time of the analysis is very short (30 min ~ 2 h). Quickness is one of the most important attributes in analytical science. Shave-off SIMS enables quicker processing and does not have the several disadvantages of conventional SIMS.

Two-dimensional mapping (XY plane) is achieved in shave-off SIMS by using the positional information of the scanning primary ion beam [4]. However, the information of Z axis is not acquired at all (Fig. 2a). If it is possible to magnify the shave-off cross-sectional ion

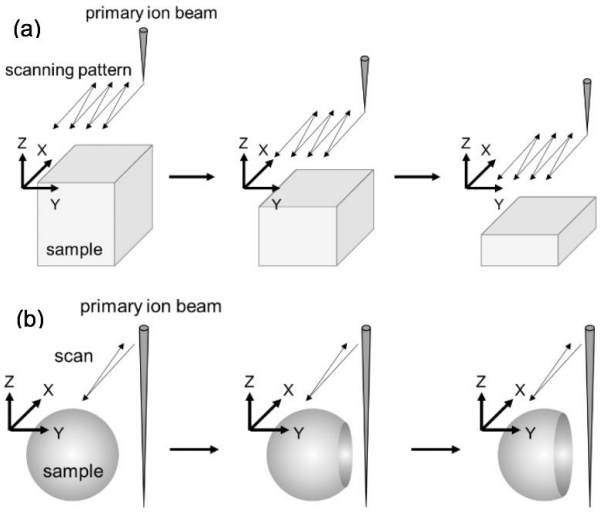

Fig. 1 Procedure of scanning (a) Conventional SIMS (b) Shave-off SIMS.

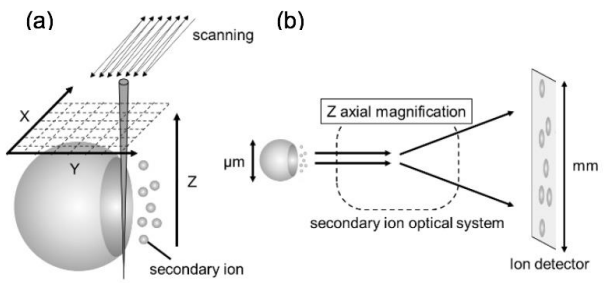

Fig. 2 (a) Simplified image of mapping in shave-off SIMS (b) Plan of Z-axial magnification.

image in the Z axis in the secondary ion optical system, three-dimensional (3D) shave-off SIMS is achieved by the combination of XY-positional information and Z-axial magnified image [5] (Fig. 2b). 3D shave-off SIMS has all the advantages of the existing shave-off SIMS. If the depth resolution and transmission of 3D shave-off SIMS become similar to those in conventional SIMS, 3D shave-off SIMS will be an attractive analytical method. In this paper, we designed the appropriate secondary ion optical system to attain the Z-axial magnification by the simulation of electric field.

2. Simulation

We used SIMION [6] to simulate the secondary ion optical system. The system consisted of the following parts: specimen, accelerating electrode and extracting electrode (extracting system), aperture, focusing lens, magnifying lens, electric analyzer, and magnetic analyzer (Mattauch–Herzog-type mass analyzer [7]) (Fig. 3a). Two datasets for the secondary ion conditions were used. One was similar to that in conventional SIMS: secondary ions were randomly emitted from a point like a cone whose half angle was 60º, and the secondary ion energy was 1–30 eV [8] (Fig. 3b). Here, we defined conventional SIMS as SIMS in which O^+, Cs^+, or other commonly used ions are employed as primary ions and they just sputters the sample surface. We used the conventional condition to confirm the function of the designed secondary ion optical system. The other dataset was the shave-off condition calculated by Trim [9]. The Trim simulation was made under the condition similar to shave-off SIMS [10-11] (Fig. 3c). The conditions of this simulation were the following: the incident ions were Ga,

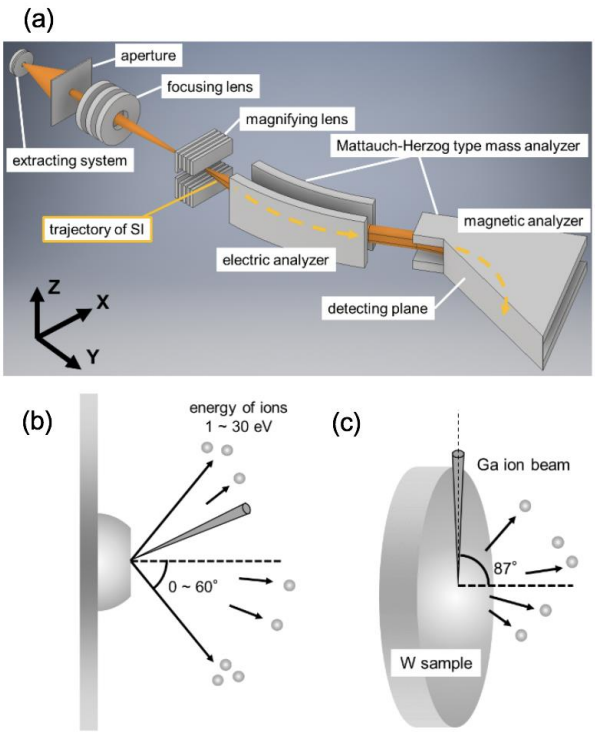

Fig. 3 (a) Secondary ion optical system. The geometrical relationship is not correct. (b) Typical SIMS conditions (c) Simplified image of Trim simulation under the condition similar to shave-off SIMS. (color online)

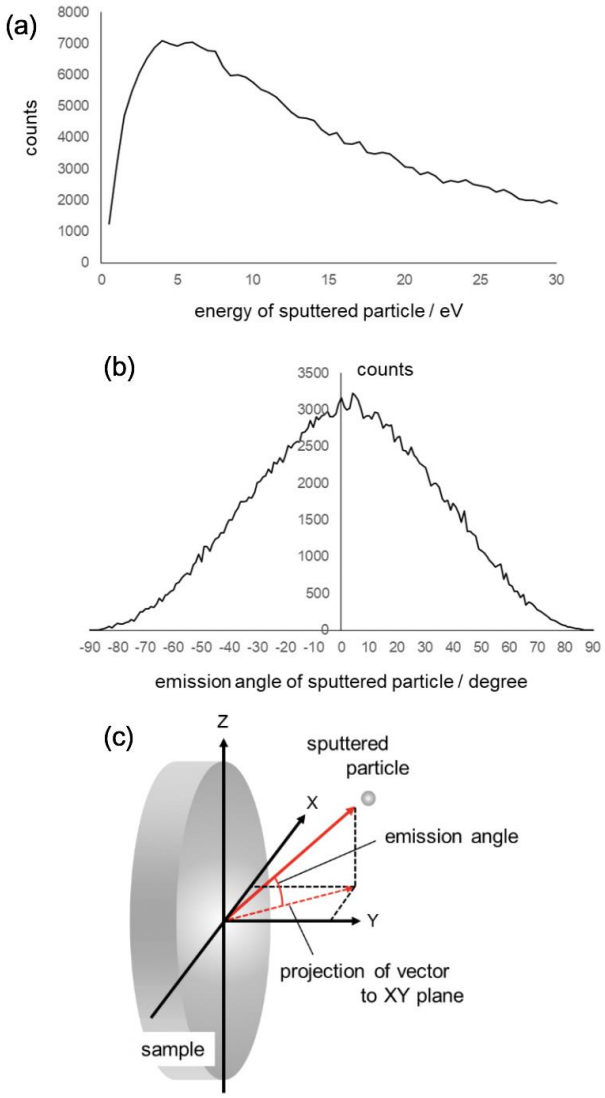

Fig. 4 (a) Energy distribution of secondary ions simulated by Trim. The Trim simulation was carried out under the condition similar to shave-off SIMS. (b) Emission angle distribution of secondary ions simulated by Trim. The Trim simulation was carried out under the condition similar to shave-off SIMS (c) Definition of emission angle. (color online)

the number of incident ions was 10^5, the energy of incident ions was exactly 30 keV, the incident angle was 87º, and the sputtered sample was W. In this simulation, sputtered particles whose energy was less than 30 eV were the secondary ions. The energy distribution and emission angle distribution of the used data is shown in Fig. 4a and 4b, respectively. The definition of emission angle is shown in Fig. 4c. We used the condition simulated by Trim to evaluate the abilities of the designed secondary ion optical system under the shave-off condition.

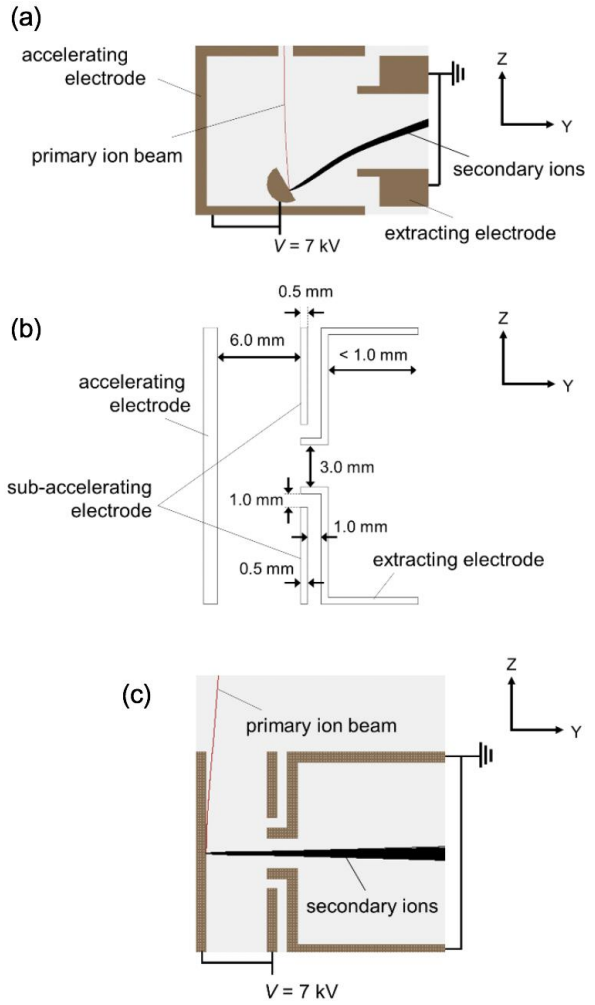

Fig. 5 (a) YZ cross-sectional image of the current extracting system. This image was drawn by SIMION. (b) Geometrical conditions used in the simulation as the new extracting system. This image was just the YZ cross section, and the three-dimensional structure was rotationally symmetric. (c) YZ cross-sectional image of the new extracting system. This image was drawn by SIMION. (color online)

3. Results and Discussion

In this paper, we first improved the extracting system and designed the magnifying lens. The required abilities of the extracting system were as follows: the rotational symmetry of the optical system was sufficiently high to satisfy paraxial approximation [12], the chromatic aberration of the secondary ions was sufficiently small to project the resolvable secondary ion image, the primary ion beam hit the sample, and the manipulation of the SIMS apparatus was easy. We improved the extracting system because the existing extracting system did not have a symmetrical structure and did not satisfy paraxial approximation (Fig. 5a). We did not acquire any

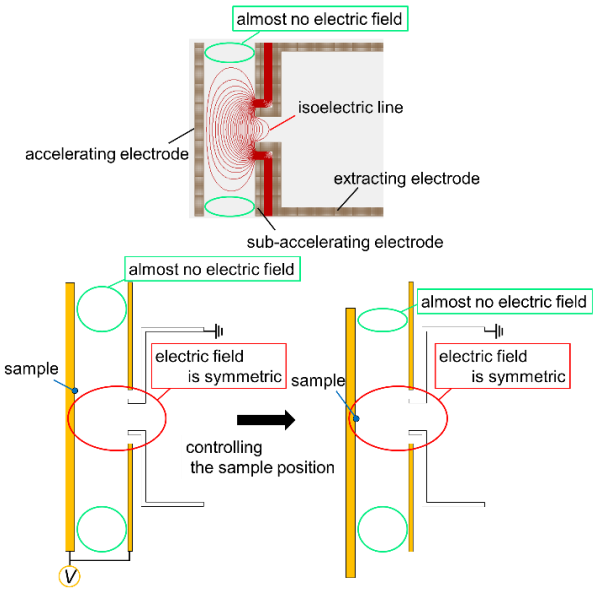

Fig. 6 Electric field and the position controlling of the sample in the new extracting system. The upper image was drawn by SIMION. The lower image was the simplified scheme of the position controlling of the sample. (color online)

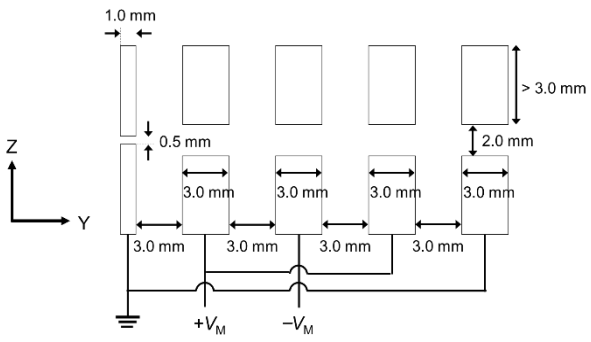

Fig. 7 YZ cross-sectional image of the magnifying lens. $\pm V_M$ is the applied voltage.

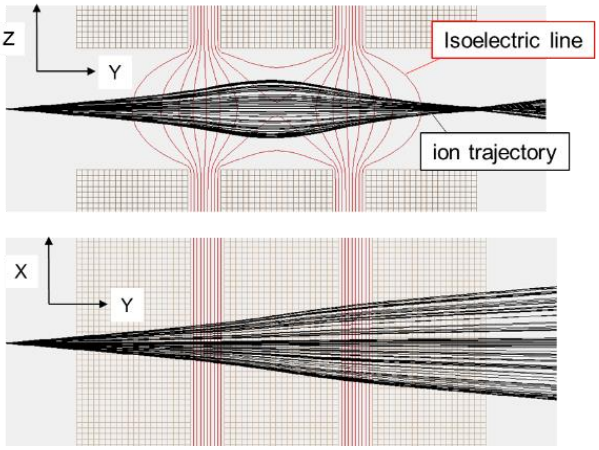

Fig. 8 Function of the planar lens. Both images were drawn by SIMION. (color online)

resolvable cross-sectional ion image by using the existing extracting system. The geometrical conditions of the new extracting system are shown in Fig. 5b. This system was constructed using the accelerating electrode, sub-accelerating electrode, and extracting electrode. The new extracting system had rotational symmetry and satisfied the paraxial approximation. In addition, the chromatic aberration became sufficiently small to resolve the cross-sectional ion image on the detector. It succeeded in reducing the bending of the primary ion beam and made the ion beam hit the sample (Fig. 5c). In Fig. 5c, the applied extracting voltage was 7.0 kV, and the energy of the primary ion beam was 30 keV. In this research, the applied extracting voltage was always fixed to 7.0 kV. We assumed that the sample is attached on the accelerating electrode directly. When the accelerating electrode position is changed to control the sample position, the rotational symmetry of the extracting system is broken (Fig. 6). However, the electric field around the sample is kept symmetric if the diameters of the accelerating electrode and sub-accelerating electrode are sufficiently large (we assumed over 20 mm) (Fig. 6). Thus, the manipulation of the new extracting system was easy.

The required abilities of the magnifying lens were as follows: the Z-axial magnification was possible, the magnification was sufficiently large to detect (from 1 μm to 0.1–1 mm), the lens effect worked only in the Z axis to satisfy the geometrical condition of Mattauch-Herzog-type mass analyzer, and the electrode structure was practical. We developed the planar magnifying lens shown in Fig. 7. In this research, we always fixed the applied voltage V_M at 1.7 kV. The electric field generated by the planar lens worked only in one direction (Fig. 8). This magnifying lens was placed at the main slit, which was part of the Mattauch–Herzog-type mass analyzer. The procedure of magnification in the designed secondary ion optical system is shown in Fig. 9. First, the real image was made at the center of the main slit. Then, the real image was magnified by the magnifying lens, and finally the magnified image was projected on

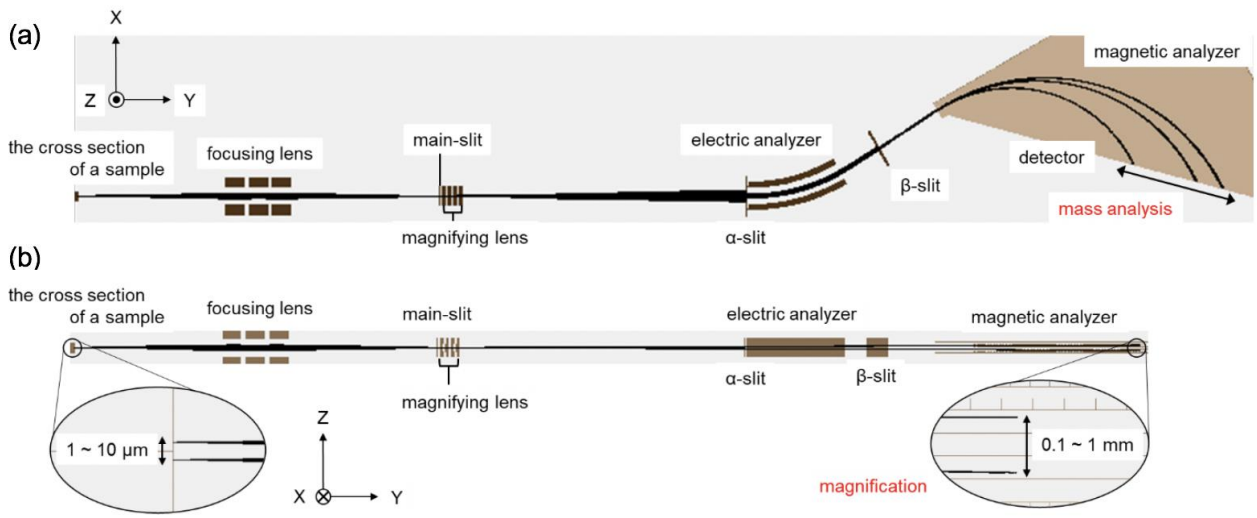

Fig. 9 Trajectory of the secondary ions in the designed secondary ion optical system. These images are different from the real simulation. These images were drawn by SIMION. (a) XY image of the trajectory. (b) XZ image of the trajectory. (color online)

the detector.

In this paper, we defined magnification ratio, Z-axial resolution, and transmission. First, the center of the cross section of the sample was set at the origin point of the simulation space. The secondary ions emitted from point-A, whose Z position was $Z_{initial}$ on the cross section of the sample, made the distribution P ($Z_{initial}$) on the detector. We defined $Z_{detected}$ as the average value of P ($Z_{initial}$). Here, it was assumed that the following equation was established.

$$Z_{\mathbf{detected}} = M * Z_{\mathbf{initial}} + C$$

where M and C were real constants. We defined the absolute value of M as magnification ratio. In addition, we defined σ as the standard deviation of P ($Z_{initial}$). Then, the value R was calculated by the following equation:

$$R = \frac{2\sigma}{|M|}$$

We defined R as Z-axial resolution. It was assumed that the number of secondary ions emitted from point-A was $N_{initial}$ and the number of secondary ions that reached the detector was $N_{detected}$. Then, the value T was calculated by the following equation:

$$T = \frac{N_{\mathbf{detected}}}{N_{\mathbf{initial}}}$$

We defined T as transmission.

In this research, we fixed the voltages that were applied to each electrode in the designed secondary ion optical system. The fixed voltages were set to optimize the Z-axial resolution when the voltage applied to the extracting system was 7.0 kV. The result of Z-axial magnification in the designed secondary ion optical system is shown in Fig. 10a, 10b. In the conventional condition, the following values were achieved: magnification ratio 1.6×10^2, Z-axial resolution 1.4 μm, and transmission 0.19% (Fig. 10a). From this result, we confirmed the function of the designed secondary ion optical system. Then, we evaluated the abilities of the designed system. The magnification ratio 1.6×10^2 was sufficient because we could magnify the cross-sectional ion image from 1 μm to 0.1 mm by using the designed secondary ion optical system. However, the Z-axial resolution 1.4 μm and transmission 0.19% was much inferior to conventional SIMS. Further improvements in the secondary ion optical system are necessary.

In the condition simulated by Trim, the following values were achieved: magnification ratio 1.6×10^2, Z-axial resolution 1.4 μm, and transmission 0.32 % (Fig. 10b). We expected the secondary ion optical system to show different results in different conditions. However, the acquired value of each physical quantity except for the transmission was same between the two datasets. The condition simulated by Trim had the unique energy and emission angle distribution (Fig. 4a, 4b). We explored why the deviation of the distribution effected the transmission and why the magnification ratio and Z-axial resolution did not depend on the distribution. Here, the aperture was set just posterior to the extracting system in the designed secondary ion optical system, and only some part of the secondary ions could pass the aperture (Fig. 3a). Thus, the transmission was mainly determined by the aperture in the designed secondary ion optical system. We concluded that the transmission changed depending on the energy and emission angle distribution of the secondary ions because the number of secondary ions passing the aperture changed depending on the distribution. On the other hand, the magnification ratio depended only on the voltages applied to each electrode

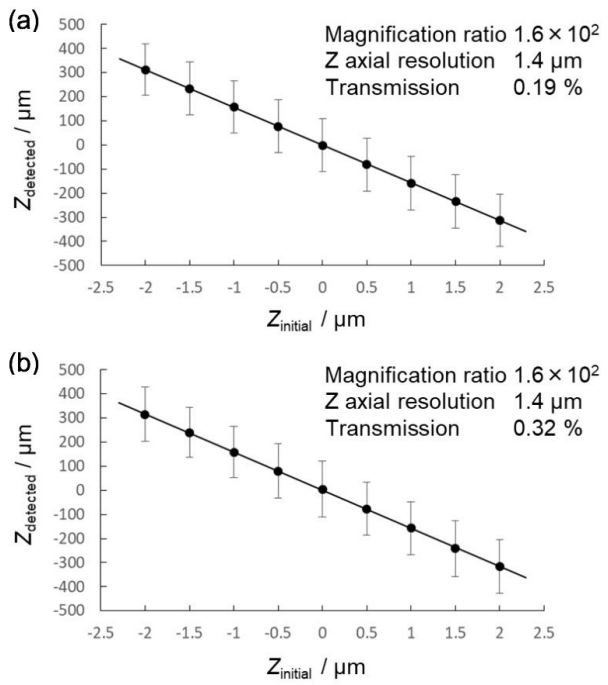

Fig. 10 Result graphs of the Z axial magnification in each condition. The error bars show 1σ section. The definition of each physical quantity follows the body. (a) Familiar condition in conventional SIMS. (b) Calculated condition by Trim.

in the designed secondary ion optical system. Moreover, we assumed that the cause of the consistency of the Z-axial resolution between the two datasets was that the distributions of the secondary ions passing the aperture were almost the same between the two datasets.

4. Conclusion

By developing the new extracting system and the magnifying lens, we suggested a new secondary ion optical system that enables 3D shave-off SIMS. The Z-axial image of samples were magnified from micrometer size to millimeter size by using this optical system. However, it is necessary to improve this optical system because the Z-axial resolution and transmission shown in this research are much inferior to that in conventional SIMS. In addition, to enhance the accuracy of the simulation, experimentally measuring the initial conditions of secondary ions in shave-off SIMS is required.

5. Acknowledgement

This work was supported by JSPS KAKENHI Grant Number 16H03814.

6. References

[1] H. Satoh, M. Owari and Y. Nihei, *J. Vac. Sci. Technol. B* **6**, 915 (1988).

[2] M. Fujii, K. Nakamura, Y. Ishizaki, M. Nojima, M. Owari and Y. Nihei, *Appl. Surf. Sci.* **255**, 1354 (2008).

[3] M. Nojima, A. Maekawa, T. Yamamoto, B. Tomiyasu, T. Sakamoto, M. Owari and Y. Nihei, *Appl. Surf. Sci.* **252**, 7293 (2006).

[4] D. Shirakura, B. Tomiyasu and M. Owari, *e-J. Surf. Sci. Nanotech.* **14**, 179 (2016).

[5] A. Habib, H. Asakura, M. Fukushima, S.-H. Kang, Y. Kim, B. Tomiyasu and M. Owari, *J. Surf. Anal.* **24**, 159 (2017).

[6] D. A. Dahl, *Int. J. Mass Spectrom.* **200**, 3 (2000).

[7] J. Mattauch and R. Herzog, *Z. Phys.* **89**, 786 (1934).

[8] S. Bouneau, S. Della Negra, D. Jacquet, Y. Le Beyec, M. Pautrat, M. H. Shapiro and T. A. Tombrello, *Phys. Rev. B* **71**, 174110 (2005).

[9] J. F. Ziegler, M. D. Ziegler and J. P. Biersack, *Nucl. Instrum. Methods Phys. Res. B* **268**, 1818 (2010).

[10] S.-H. Kang, M. Fukushima, H. Asakura, A. Habib, Y. Kim and B. Tomiyasu, M. Owari, *J. Surf. Anal.* ***24***, 164 (2017).

[11] S.-H. Kang, K. Matsumura, T. Azuma, B. Tomiyasu and M. Owari, *J. Surf. Anal*. **25**, 165 (2019).

[12] K. Ura, *Electron and Ion Optics*, KYOITSU SHUPPAN (1994) (in Japanese).

査読コメント，質疑応答
査読者 1. 久保田 直義（日鉄住金テクノロジー）

本稿は，shave-off SIMS の適用範囲を 2 次元マッピングから 3 次元マッピングへ拡張するための装置開発に関して，シュミレーションを用いて検討した結果を示したものであり，今後の最適化に向けて有用な情報を提供しております．論文の内容を明確にするために，以下の点に関してご検討ください．

[査読者 1-1]
Fig. 3(b)で，キャプションおよび本文では“conventional SIMS”となっておりますが，図中には Fig. 3(c)と同様に“shave-off SIMS”を連想させる 1 次イオンビームのコーンが記載されております．コーンの軸と試料法線のなす角をもう少し小さくすることは可能でしょうか．

[著者]
ご指摘の通りだと思います．Fig. 3(b)を修正しました．

[査読者 1-2]
2 章の本文“The other data-set….”の文章に関しまして，8 行前の“One was the normal condition in conventional SIMS.”と呼応して，“shave-off SIMS”で受ける方が分かりやすいかと思いますが如何でしょうか．

[著者]
ご指摘の通りだと思います．“The other data-set was the shave-off condition calculated by Trim”と修正しました．

[査読者 1-3]
Trim の計算条件に関して，リファレンスに挙げられておりましたが，スパッタ粒子源は点線源でしょうか？ 本文でも 1 次イオンの入射角やスパッタ粒子を発生させた領域の情報等，少し計算条件の加筆をご検討下さい．

[著者]
Trim シミュレーションの条件を加筆しました．また，Trim シミュレーションの結果についてエネルギー分布・放出角度分布のグラフなどがあると良い，という査読者 2 の方からのご指摘がありましたので，そちらのグラフも追加しました．

査読者 2. 匿名

[査読者 2-1]
「2. Simulation」において唐突に“two data-sets”を準備する理由がよくわからないので説明すべきと考えます．その two data-sets による結果である Fig. 6† (a)と(b)は Transmission 数値の違い以外は全く同じ図であるように見える（a と b の両方を図示する意味がないように思える）．

† 掲載版の Fig. 10

[著者]
二つのデータセットを用いた理由は，本研究で設計した二次イオン光学系の性能をチェックするためです．conventional condition は，単純に二次イオン光学系の動作を確認するために用いました．一方で，Trim シミュレーションによる condition は，より shave-off 条件を再現する状況では二次イオン光学系の性能がどう変化するのかチェックするために用いています．Trim の方では conventional condition とは違い，放出二次イオンのエネルギー・角度分布が一様でなかったため，Z axial resolution や transmission に変化が生じる可能性がありました．結果として transmission 以外はほぼ変化がなかったのですが，グラフも二つ示しています．この部分についての記述・考察がなかったため，Result and Discussion にも記述を追加しました．

[査読者 2-2]
「3. Results and Discussion」節の 2〜8 行目で“The required abilities of the extracting system were the following: the rotational symmetry of the optical system was high, the chromatic aberration of the secondary ions was small, the primary ion beam could hit the sample, and the manipulation of the SIMS apparatus would be easy.”と書かれていますが，どの程度“high”や“small”なのでしょうか？ またそれをどう考慮して Fig. 4 や Fig. 5 の設計を行ったのでしょうか？

[著者]
イオン光学系における結像特性を良くするためには，幾何収差と色収差の二つを小さくする必要があ

ります．幾何収差を小さくするためには，近軸近似を満足するように系の対称性を高くすることが不可欠です．特に，extracting system においては回転対称系が最も対称性が高くなります．この部分については加筆しました．一方，色収差に関しては，設計上は重要ですが既存のシステムと本研究で設計したシステムでは，おそらくですが，あまり違いがありません．既存のシステムでは幾何収差が大きすぎて色収差の影響がわからない，ということも挙げられます．この部分については，「分解可能な二次イオン像が投影できる程度に色収差が小さい」というように加筆しました．定量的な評価は非常に難しいため，本稿では色収差について特に記述した部分はありません．

既存のシステムにおける問題点と設計したシステムの利点について加筆しました．

[査読者 2-3]

「3. Results and Discussion」節で“The geometrical conditions used in the simulation were shown in Fig. 4b, which could be changed depending on the situations.”とありますが，「どんな状況」によって「何を変えられるのか」丁寧に説明してください．

[著者]

引出系の扱いについて加筆しました．まず，引出系に含まれている押出電極に試料をくっつけるような形で固定することを考えています．その状態において試料が一次イオンビーム走査視野の中にない場合や，二次イオン光学系の光軸上に試料がない場合には押し出し電極ごと試料を移動させる必要があります．このとき，系全体としては対称性が破れてしまいますが，高電圧（本項では 7 kV の電圧を印加した）が印加された電極を十分大きくとる（設計した引出系だと半径 20 mm 以上という程度）ことで，二次イオンの飛行軌道に影響のある領域における電場の対称性は保たれます．

既存の引出系には結像性がまったくなかったため，グラフの作成も行っていません．そのため，既存の引出系と設計した引出系の定量的な比較はしていません．それについても加筆しました．

[査読者 2-4]

「3. Results and Discussion」節の “magnifying lens”に必要な性能についても説明が不足しています．また“the magnification was large enough to detect”とはどの程度大きければ良いのでしょうか？ Fig. 2(b)で「μm」を「mm」に拡大するような模式図がありますので，それならば 1000 倍程度の拡大率が必要ということでしょうか？

[著者]

説明を加筆しました．Fig. 2 の描写はイメージであり，実際の拡大率は 100 倍程度でも問題ないと思われます．特に，本研究で用いることを想定した検出系は Z 軸方向の幅が 5 mm，検出器の分解能が 40 μm となっていたので，実際に 1000 倍の拡大率を実現すると分析対象が制限される可能性がありました．今後，より大きな拡大率を得ることを目標とするのも必要になる可能性はありますが，現時点では十分な拡大率が得られたと考えています．

[査読者 2-5]

「3. Results and Discussion」節で“We developed the planar magnifying lens shown in Fig. 5† to satisfy the requirements”とありますが，なぜこのような電極配置であれば平面的に拡大できるのかの説明がありません．それがわかるような説明を本文中に記述する，もしくはそれが明快にわかるような SIMION のトラジェクトリー結果等があれば提示してください．また$+V_M$ と$-V_M$ と正負で同じ電圧を印加したようですが，何ボルトの電圧を印加したのでしょうか？ なお Fig. 5† (b)の図については必要性を感じないのですが，必要でしょうか？

† 掲載版の Fig. 7

[著者]

平板型レンズによるレンズ作用の様子を SIMION で描画したものを図として追加しました．

$+V_M$，$-V_M$の値はV_M = 1.7 kV です．これも加筆しました．

Magnifying lens の XY 投影図ですが，回転対称ではなく平板型である，ということを強調するために示しました．しかし，SIMION によるトラジェクトリーの図と本文での記述を追加したため，十分に意図が伝わると判断し，ご指摘のように削除しました．

[査読者 2-6]

どの程度の Magnification ratio，Z axis resolution，transmission efficiency を目指しているのか，以前の

system と比較して新設計の system ではどの程度それらの値が改善されたのかについても説明するようにしてください.

[著者]

結論から申しますと，本研究での一番の目的は「Z 軸方向に拡大された二次イオン像を得ること」であり，定性的に「拡大・結像」ができた時点で成果としました．そのため，本研究においては，magnification ratio や Z axial resolution についての具体的な目標は定めていませんでした．最終的な目標は，修正後の 1. Introduction 末尾に書きました通り，「従来の SIMS に追いつくこと」です．原理的に ultra-shallow SIMS には追い付けないと思われますので，具体的には 10^2 nm のオーダーを目指しています.

本研究では，二次イオン光学系の設計を最優先の目的としたため，引出電圧の条件検討はせず，引出電圧 7.0 kV（固定）を前提としました．当研究室の装置の都合を考慮した結果，この値となっています.

そのうえで magnifying lens の印加電圧 V_M について条件検討を行っています．また，本研究では V_M の値は Z axial resolution を最小にするように決定しました．ご指摘の通り，引出電圧や V_M の条件が変動すれば magnification ratio や Z axial resolution も変動します.

‘two data-sets’の違いによる結果の変化については考察を追加しました．transmission の違いは，引出系の直後段に配置されたアパーチャーによって主に決定されており，二次イオンのエネルギー・放出角度分布によってアパーチャーを通過するイオンの数が変化するため 2 つのデータセット間で結果が異なったと考えられます．一方，magnification ratio は二次イオン光学系の各電極に印加された電圧に依存するため分布には依存しません．また，Z axial resolution はアパーチャーを通過した二次イオンの分布が 2 つのデータセットで差がなかったために同じ値になったのだろうと推測されます.

修正後の 3. Results and Discussion 11 ~ 15 行目に書きました通り，以前のシステムでは検出面において試料断面の二次イオン像が全く結像されなかったため（質量分解はされるが Z 軸方向の情報が全く得られなかった，という意味です），定量的な比較は難しいかと思われます．’we improved the extracting system’という表現を用いましたが，～倍，という指標で比較できるレベルの改善ではありません．この点に関する記述も，修正後の 3, Results and Discussion 1 段落目に追加しています.

[査読者 2-7]

「6. References」の[12]も英訳してください.

[著者]

ご指摘ありがとうございます．英訳しました.